



Published in final edited form as:

Noise Control Eng J. 2015 ; 63(2): 159–168.

## Identification of Noise Sources and Design of Noise Reduction Measures for a Pneumatic Nail Gun

Vignesh Jayakumar<sup>a</sup>, Jay Kim<sup>b</sup>, and Edward Zechmann<sup>c</sup>

Vignesh Jayakumar: jayakuvh@mail.uc.edu; Jay Kim: kimj@ucmail.uc.edu; Edward Zechmann: cri6@cdc.gov

<sup>a</sup>Dept. of Mechanical and Materials Engineering, University of Cincinnati, Ohio – 45221

<sup>b</sup>Dept. of Mechanical and Materials Engineering, University of Cincinnati, Ohio – 45221

<sup>c</sup>National Institute of Occupational Safety and Health, Cincinnati, Ohio – 45226

### Abstract

An experimental-analytical procedure was implemented to reduce the operating noise level of a nail gun, a commonly found power tool in a construction site. The procedure is comprised of preliminary measurements, identification and ranking of major noise sources and application of noise controls. Preliminary measurements show that the impact noise transmitted through the structure and the exhaust related noise were found to be the first and second major contributors. Applying a noise absorbing foam on the outside of the nail gun body was found to be an effective noise reduction technique. One and two-volume small mufflers were designed and applied to the exhaust side of the nail gun which reduced not only the exhaust noise but also the impact noise. It was shown that the overall noise level could be reduced by as much as 3.5 dB, suggesting that significant noise reduction is possible in construction power tools without any significant increase of the cost.

## 1 INTRODUCTION

Noise-induced hearing loss (NIHL) is one of the most frequently reported job-related illnesses in the United States. As more than 2.9 million construction workers are exposed to harmful levels of noise<sup>1</sup>, hand held power tools that emit high intensity operating noises are one of the major contributors to occupational NIHL. While various noise guidelines define the exposure limit and recommend necessary protections to prevent hearing losses of workers<sup>2–5</sup>, reduction of the operating noise itself is always desirable. The motivation of this study is to demonstrate that a significant reduction of the operating noise of construction tools can be achieved by relatively simple design modifications with little increase to the cost of the tool. A pneumatic nail gun, one of the common power tools that emit high-intensity noise, was selected for the demonstration. The selected nail gun generates a train of

Correspondence to: Jay Kim, kimj@ucmail.uc.edu.

### DISCLAIMER

The findings and conclusions in this report are those of the author(s) and do not necessarily represent the views of the National Institute for Occupational Safety and Health. Mention of any company or product does not constitute endorsement by the National Institute for Occupational Safety and Health (NIOSH). In addition, citations to Web sites external to NIOSH do not constitute NIOSH endorsement of the sponsoring organizations or their programs or products. Furthermore, NIOSH is not responsible for the content of these Web sites. All Web addresses referenced in this document were accessible as of the publication date.

high-level impulsive noises, that instantaneously reach a peak level of up to 120-dBA (re: 20 $\mu$  Pa) at the operator's ear position.

ISO 11688-1 and ISO 11688-2 provide detailed information on planning the physics for low noise design<sup>6-7</sup>, although each tool will require a different solution for noise reduction, a general iterative procedure can be employed as follows.

1. Examine the mechanism and operation of the tool to identify potential noise sources and transmission paths.
2. Assess contributions of the noise sources and transmission paths to the overall noise level to identify major contributors.
3. Develop designs that can lower contributions of major noise sources.
4. Evaluate and compare performances of modified designs

The measurement procedure in this paper was designed carefully to reflect actual operation of the tool while minimizing measurement errors and uncertainties and ensuring the repeatability of the tests. The noise maps were captured by an acoustic camera with a 48 channel microphone array with a 35 cm diameter model Sphere 48-35 AC Pro manufactured by Gesellschaft zur Förderung angewandter Informatik (GFAI), Berlin Germany and operated by Sage Technologies Walled Lake, MI. These were used to identify major noise sources and their transmission paths. The total A-weighted sound power of the tool was used for comparison. A 10-microphone system was employed to measure the total A-weighted sound power of the tool. Because of the highly transient nature of the event, time histories of the noise captured multiple times were post-processed to obtain the sound power and other frequency domain information.

## 2 OPERATING MECHANISM AND NOISE SOURCES

### 2.1 Operating Mechanism of the Nail Gun

The operating mechanism of the nail gun is examined to identify potential noise sources and their transmission paths. Fig. 1 shows the basic construction of the nail gun selected in this study. Fig. 2 illustrates the air manifold system of the nail gun that drives the nail and the plunger and piston mechanism. The hatched areas in Fig. 2 indicate the plenums filled with high-pressure air. The plunger acts as a large valve which opens very quickly to send high pressure air to propel the piston and piston rod forward to drive the nail. Fig. 2 (a) shows the idle status before the trigger of the nail gun is pulled, in which the mechanical spring is in its natural length. The plunger remains stationary because the total pneumatic force acting on it is zero. Once the trigger is pulled, the trigger valve is closed as shown in Fig. 2 (b), cutting off the high-pressure air above the plunger and pushing the plunger upward and compressing the mechanical spring. This opens up the path for the compressed air to rush into the main cavity, and the high-pressure air pushes the piston and the piston rod downward to drive the nail into the wood. At the end of the stroke, the exhaust port opens to move the high-pressure air out. The trigger is released after the shooting of the nail, which opens the trigger valve again. Due to the force from the compressed spring, the plunger returns to the position shown in Fig. 2 (a), which cuts off the supply of compressed air to the main cavity. The

compressed air stored in a small storage volume and a bleeder hole below the piston pushes the piston back into the position shown in Fig. 2 (a). The process repeats when the trigger is pulled again.

## 2.2 Identification of Major Noise Sources and Transmission Paths

Fig. 3 shows a time history of the sound pressure measured for one operation cycle of the nail gun. The time history is matched with noise maps obtained by an acoustic camera that show the areas of the noise emission of high intensity. The time window of the acoustic camera was set to be 2.82 milliseconds. From an investigation of the sound pressure time history and noise maps in conjunction with the operating mechanism of the nail gun, the possible noise sources and transmission paths are listed as shown in Table 1. Based on the information available, the four major noise generation mechanisms corresponding to the four distinct peaks in the time history can be identified as follows.

- A. Noise generated by the air movement through the manifold: The air rushing into the cavity around the plunger to build up pressure causes unsteady gas pulsations in the manifold. The manifold that involves this air movement is completely enclosed; therefore the noise induced by the air movement is considered much lower in this stage than those in other stages.
- B. Noise generated by the impact between the piston rod and the nail: The impact noise generated in the annular cavity inside the Cylinder Piston (Part 3 in Fig. 1) is transmitted through the double cylinder walls in the Cylinder Piston and Body Side Cover (Parts 3 and 2 respectively in Fig. 1) and through the Body Top Cover (Part 1 in Fig. 1). Double walls provide a significant transmission loss, especially in the high frequency range [8]. Therefore in this stage, the small opening for the exhaust air in the Body Top Cover (Part 1 in Fig. 1) provides the major transmission path in this stage. The noise map (B) in Fig. 3 supports this observation.
- C. Impact noise generated when the nail strikes the wood: The sound in this stage is shown in the color map (C) in Fig. 3. Reducing noise at this stage was not investigated.
- D. Noise due to the compressed air released through the exhaust port: The compressed air is discharged to the ambient through a port on the top cover of the tool. This intermittent flow induces unsteady gas pulsation noise. As an unintended consequence of the design, the port radiates the impact noise in the cavity inside of the tool case as well. A reactive muffler can be designed to reduce gas pulsation noise and the impact noise explained in (B) by reducing the effective area of the noise radiation.

A similar observation was made in previous works<sup>9–11</sup>.

## 3 MEASUREMENT OF THE SOUND POWER

Theoretically sound power is independent of the measurement location and measurement conditions. In laboratory controlled sound power measurements in accordance with ISO 3744, the source location must be within a reference box, and the measurement conditions

are controlled which optimizes repeatability of the measurements. Therefore sound power is an effective metric for comparing the baseline tool performance with the performance of the modified designs. The total A-weighted sound power and the A-weighted 1/3 octave sound power spectrum were utilized in this study.

### 3.1 Measurement Setup

A ten-microphone system (shown in Fig. 4) was used to measure the sound power using the standard ISO 3744:2010<sup>12</sup>. Using ISO 3744 Annex B Table 2 positions 1 through 10, ten microphones are distributed on the surface of a 2-meter radius hemisphere. Each microphone covers an equal area on the surface of the hemisphere. The nail gun fired nails downward on two 2"×4" wooden blocks positioned horizontally on top of each other in a sand box that was located at the center of the hemisphere. Because it is difficult to fire nails with an equal time interval, measurements were made of a single nail firing. The measurements were repeated several times, post-processed in the frequency domain and averaged.

For all measurements, a 1.0 second time window and a sampling rate of 100 kHz were used, which provided a Nyquist frequency of 50 kHz and 1.0-Hz resolution for the frequency domain analysis. A trigger was set up so that the time history of the sound pressure is measured from 300 milliseconds prior to the impact for the duration of 1.0 second.

To further reduce the effects of variations on each sound power measurement, the pressure time histories were measured with the operator in two different positions, position 1 and position 2 shown in Fig. 4, ten measurements from each side. After finishing ten rounds of measurements at position 1, the position of the operator and nail gun was rotated 180 degrees, and another ten measurements were taken from Position 2. The sound power for the 20 measurements obtained is averaged to further minimize the effects of the directivity of the tool noise and event-to-event variations.

### 3.2 Calculation of the Sound Power

The A-weighted and 1/3 octave band sound power levels were determined according to the procedures in ISO 3744 from the sound pressure measurements at each microphone. The sound power level is obtained as;

$$L_w = 10 \log_{10} \frac{W}{W_{ref}} \quad \text{Eqn. 3-1}$$

where,  $W_{ref} = 10^{-12}$  watts<sup>13-14</sup>.

Sound power spectrum can be obtained as a function of frequency in any constant or proportional band format by adding the frequency components of the sound power described by Eqn. 3-1 within the frequency bands. Averaging of 20 measurements also is conducted by averaging the sound power.

In this study, the A-weighted 1/3 octave band sound power levels were primarily used for comparison. Fig. 5 shows the A-weighted 1/3 octave band sound power levels of the nail

gun before any modification (Baseline – Complete Time History). The sound power spectra of the strike and exhaust period can be obtained by digitally separating the peaks in the time histories as shown in Fig. 3, zero padding the rest of the 1 second long data and applying signal processing to the resultant time histories. Fig. 5 also shows the sound power spectrum of the exhaust period only (Baseline – Exhaust only) and the sound power spectrum of the impact period (Baseline – Strike only).

## 4 APPLICATION OF NOISE CONTROL MEASURES

### 4.1 Effect of Noise Radiation Surface

In Fig. 1 the Body Bottom Cover, Body Side Cover and Body Top Cover, parts 4, 2, and 1 are referred to as Zone 1, Zone 2 and Zone 3 respectively. These three zones have large surface areas that radiate noise<sup>15-16</sup>. Relative contributions of these areas to the total noise level were estimated by wrapping foam on the surface in Zone 1, 2 and 3, one at a time. The results clearly indicate that significant reduction in sound power levels can be achieved by addressing the structural vibrations of the nail gun body (Zone 1, 2 and 3) and the exhaust noise. The contribution of the former on the overall noise is however seen to be greater than the latter. Fig. 6 and Fig. 7 highlight 1/3<sup>rd</sup> octave band sound power comparisons for the strike related and exhaust related noise for the trials with noise isolations applied to Zones 1, 2, 3, and the exhaust noise.

### 4.2 Effect of Exhaust Noise

To evaluate the contribution of the exhaust noise to the overall noise levels, the noise of the tool was measured after the exhaust flow was ducted away by using a hose of 3/8-inch diameter and 4 ft 10 inches long with a dissipative muffler at the end. This reduced the  $L_{WA}$  during the exhaust period (see Fig. 7) by about 6 dBA, but the total  $L_{WA}$  (exhaust + strike) only by about 2 dBA.

### 4.3 Effect of Exhaust Mufflers

Small volume mufflers can be designed by using a lumped parameter modeling approach that models the muffler manifold composed of Helmholtz resonators. The four-pole method can be used very conveniently for this purpose<sup>17-18</sup>. The pneumatic nail gun used in the trials had an average flow rate of approximately 36 m/s. The Mach number associated with such a flow ( $M \approx 0.1$ ) is small enough to ignore the effect of the mean flow.

The characteristic of an acoustic system, an exhaust muffler in this case, can be represented in the frequency domain as follows.

$$\begin{Bmatrix} \mathbf{Q}_{in} \\ \mathbf{P}_{in} \end{Bmatrix} = \begin{bmatrix} A & B \\ C & D \end{bmatrix} \begin{Bmatrix} \mathbf{Q}_{out} \\ \mathbf{P}_{out} \end{Bmatrix}, \quad \text{Eqn. 4-1}$$

where,  $\mathbf{Q}_{in}$ ,  $\mathbf{P}_{in}$  are the amplitudes of the volume flow and pressure at the input point,  $\mathbf{Q}_{out}$ ,  $\mathbf{P}_{out}$  are the amplitudes volume flow and pressure at the output point, and A, B, C, D are the four pole parameters of the overall muffler system. All these variables are complex quantities. The procedure to obtain these system four pole parameters is explained in

Appendix A. It can be considered  $P_{out} \approx 0$  with the end correction at the tail pipe; therefore the transfer function (TF) between the input and output sound power is;

$$TF = 10 \log_{10} \left| \frac{Q_{out}}{Q_{in}} \right|^2 = 10 \log_{10} |A|^2 (dB). \quad \text{Eqn. 4-2}$$

The positive TF values indicate that the noise is amplified, similarly the negative TF values indicate the noise is reduced. The TF in this definition can be understood roughly as the negative of the insertion loss; therefore negative value of TF in dB can be interpreted as the reduction of the sound power in dB directly related to the gas pulsation.

Fig. 8 shows the TFs calculated for the four different muffler designs shown in Fig. 9 through Fig. 12, using the TF function defined in Eqn. 4-2. The low pass filter effect of a muffler system is clearly seen in this. The muffler design amplifies noise in and around the peaks (resonance frequency) in the Transfer function plot. Beyond the cut-off frequency, about 1.4 times of the resonance peak, the transfer function becomes negative indicating attenuation of sound beyond this cut-off frequency. The design parameters, volumes and lengths of the pipes, are shown in Table 2. The TF plot for different muffler dimensions can be used to design the muffler to arrive at the best combination of dimensions to achieve the lowest possible cut-off frequencies. Mufflers shown in Fig. 9 and Fig. 10 are single volume mufflers, while those shown in Fig. 11 and Fig. 12 are two-volume mufflers with the volumes connected serially and as a side-branch respectively.

#### 4.4 Comparison of Results

The sound power analysis was carried out by demarcating the collected data as strike related and exhaust related, although the two noises could not be completely separated. The trace of the strike related energy in the exhaust spectrum is quite clear from the reduced total sound power levels for exhaust related noise in the trials involving only foam wrapping on the nail gun body in Table 3 shows the A-weighted sound power spectrum of the tool measured with foam wrapping in Zone 3 as the only noise control measure. Fig. 13 shows the A-weighted 1/3 octave band sound power level for only Zone 3 covered in acoustic foam. A reduction in noise levels is observed in two frequency ranges indicated as 'A' and 'B' in the figure, showing a broadband effect as expected.

Fig. 14 shows the effect of Muffler 1 with variable tail pipe lengths. These comparisons are presented in the unweighted sound power format to highlight the regions of attenuation and amplification. It is seen that the single volume muffler, with a tail pipe of 0.025 m length, amplifies the flow pulsation noise near its resonance frequency and attenuates noise from and after a little beyond this region. As expected, the increase in tail pipe length causes a decrease in the resonance frequency and cut off frequency of the muffler. The increase in the amplitude of the frequency components below 200 Hz is believed to be caused by mechanical vibration of the tail pipe. This is mainly because of the rattling of the muffler caused by the exhaust flow on the plastic muffler components.

An interesting and worthwhile observation from Fig. 14 is the significant reduction in the high frequency contents, which are primarily attributed to the impact noise. It is deduced

that the exhaust muffler reduces the opening through which impact noise radiates, resulting in the reduction of the level of high frequency components.

Table 3 summarizes effects of design variations compared to the baseline data. As it is shown, covering Zone 1, Zone 2 and Zone 3 with foam reduces the noise level by 2.6, 2.2 and 3.5 dBA respectively. However, wrapping the tool with foam is difficult to implement with a potential issue of heat build-up. Muffler 2 was designed so that it functions as a low-pass filter and also covers Zone 3. Muffler 2, in addition to reducing exhaust noise, decreases the impact noise transmission through the top and also decreases the structure borne noise by reducing Part 1 vibration. The Muffler 2 design decreases the impact noise transmitted through exhaust opening by reducing the effective opening area and also decreases the structure borne noise from Zone 3 by adding mass to the vibrating top cover (Zone 3). Because the muffler fitment is made from plastic, there is an impedance mismatch between the top cover and the muffler. A comparison of the effectiveness of Muffler 1 and Muffler 2 is presented in Fig. 15. Since, Muffler 2 has better attenuation than Muffler 1 in the low frequency range relevant to gas pulsation induced noise, further trials were conducted based on this design configuration. The effects of the different muffler configurations such as single chamber design (Muffler 2), double chamber design (Muffler 3) and single chamber with resonator side branch (Muffler 4) is highlighted in Fig. 16. Muffler 3 and 4 also offer almost equally good improvement, with slightly lower first resonance peak and cut off frequency compared to Muffler 2 design.

## 5 CONCLUSIONS

An experimental-analytical effort was used to reduce the operating noise level of a nail gun. The sound power level was used to compare the tool with different design modifications. The operating condition of the tool such as the operating pressure, flow restrictions and powering rate and the measurement set up were kept as identical as possible for accurate comparison of the performance. Preliminary measurements identified that the impact noise transmitted through the structure and the exhaust related noise were found to be the first and second major contributors. Applying a noise absorbing foam on the outside of the nail gun body was found to be an effective noise reduction technique. One and two-volume small mufflers were designed and applied to the exhaust side of the nail gun which reduced not only the exhaust noise but also the impact noise. It was shown that such low-cost measures could reduce the overall noise level of the nail gun significantly, by as much as 3.5-dB. This accomplishment suggests that significant noise reduction may be possible in many construction power tools if the overall noise level becomes a high priority of the manufacturer. Further improvements will certainly be possible if the manufacturer engineers the tool considering the noise performance from the design stage. Such techniques include, for example, applying large impedance mismatches between different layers of the structure or using viscoelastic-damping treatment in some areas of the structure<sup>13</sup>. The overall cavity design of the exhaust pathway can also be studied with regards to the design of the chambers and the bleeder holes used in the equipment to bleed the exhaust.

## Acknowledgments

We thank SENCO for providing a FramePro 601 and safety instruction and technical assistance in developing the noise controls. We are grateful to Sage Technologies of Walled Lake, MI for acquiring and analyzing data with the AC Pro Acoustic Camera. We would also like to thank INCE/USA and the INCE Foundation for providing the \$500.00 student project grant that enabled a student project study presented in Noise-Con 2013 that formed the basis of this paper. We would also like to thank those who participated in the student project: Andrew Hubbard, George Schneider, and Stephen, Louie.

## APPENDIX A – Muffler Design Analysis

Ref. [14] can be used for more detail, general discussions on the four-pole method that is described briefly here. The four-pole matrix of a small cavity is given by:

$$[V] = \begin{bmatrix} 1 & \frac{j\omega V}{\rho_o c^2} \\ 0 & 1 \end{bmatrix}$$

where,  $V$  is the volume of the cavity,  $\omega$  is the circular frequency,  $j = \sqrt{-1}$ ,  $\rho_o$  is the density and  $c$  is the speed of sound.

The four-pole matrix of a short pipe is;

$$[P] = \begin{bmatrix} 1 & 0 \\ \frac{j\omega \rho_o L_e}{S} & 1 \end{bmatrix}$$

where,  $S$  is the cross-sectional area of the pipe,  $L_e$  is the effective length of the pipe that is given by,  $L_e = L + \Delta L_1 + \Delta L_2$  where  $\Delta L_1$  and  $\Delta L_2$  are end corrections to account the radiation impedance at the end, which are 0.85 times (flanged end) or 0.6 times (unflanged end) of the radius of the pipe.

A very important and useful property of the four-pole parameter method is the cascading property. The system four pole matrix of Muffler 1 shown in Fig. 9 is obtained by multiplying three four pole matrices:  $[P_5]$   $[V_6]$   $[P_7]$ , where the subscripts indicate the element number shown in the figure.

The system matrix of Muffler 2 shown in Fig. 10 is obtained as  $[V_1]$   $[P_4]$ , and that of Muffler 3 in Fig. 11 is obtained as  $[V_1]$   $[P_2]$   $[V_3]$   $[P_4]$ . The system matrix of Muffler 4 has to be

obtained using the side branch impedance as,  $[V_1] \begin{bmatrix} 1 & \frac{1}{Z_{as}} \\ 0 & 1 \end{bmatrix} [P_4]$ , where  $Z_{as}$  is the

acoustic impedance at the side branch input point given by  $Z_{a,s} = \frac{1 - \frac{\omega^2 V_3 L_e 2}{c^2 S_2}}{\frac{j\omega V_3}{\rho_o c^2}}$ .

The four-pole method used in this paper is based on the lumped parameter modeling which is valid in the low frequency range. The small muffler dimensions justify this approach.

## References

1. NIOSH Hearing Loss Research Program Review. National Institute for Occupational Safety and Health (NIOSH); 2014. <http://www.cdc.gov/niosh/nas/hlr>
2. Occupational noise exposure standard. Vol. 48. OSHA, U.S. Department of Labor; 1983. p. 29687-29698.
3. Occupational noise exposure: Hearing conservation amendment. OSHA, Department of Labor; 1981.
4. Nail gun safety: A guide for construction contractors. NIOSH; 2011–12.
5. Safety United States and Health Topics — Occupational Noise Exposure. OSHA, Department of Labor; 2014. <https://www.osha.gov/SLTC/noisehearingconservation/>
6. Acoustics — Recommended Practice for the Design of Low-noise Machinery and Equipment — Part 1: Planning, ISO 11688-1. International Organization for Standardization; Geneva, Switzerland: 1995.
7. Acoustics — Recommended Practice for the Design of Low-noise Machinery and Equipment — Part 2: Introduction to the physics of low-noise design, ISO 11688-2. International Organization for Standardization; Geneva, Switzerland: 1998.
8. Lee J, Kim J. Analysis and Measurement of Sound Transmission Through a Double-Walled Cylindrical Shell. *Journal of Sound and Vibration*. 2002; 251(4):631–649.
9. Jayakumar, V.; Hubbard, A.; Schneider, G.; Louie, S.; Zechmann, E. Design and Evaluation of Noise Control Measures for a Pneumatic Nail Gun; Proceedings of Noise-Con.; Denver CO. Cincinnati, OH 45221: University of Cincinnati; 2013. p. 279-286.
10. Hicks, D.; Vu, K.; Rao, M. Study and Reduction of Noise from a Pneumatic Nail Gun; Proceedings of Noise-Con; Cleveland OH. Houghton, MI 49931: Michigan Technological University; 2003. p. 117-122.
11. Adelberg, J.; Anderson, R.; Kuykendall, B.; Schwartz, T.; Vu, K.; Rao, M. Study of Noise Transmission from a Pneumatic Nail Gun. ME4704 Project Report, Submitted to National Institute for Occupational Safety and Health (NIOSH) c/o Chuck Hayden and Michigan Tech c/o Dr. Mohan Rao; May. 2002
12. Acoustics. Engineering method in an essentially free field over a reflecting plane. ISO 3744, International Organization for Standardization; Geneva, Switzerland: 2010. Determination of Sound Power Levels of Noise Sources using Sound Pressure.
13. Beranek, L.; Istvan, L. Noise and Vibration Control Engineering Principles and Applications. John Wiley and Sons; 1992. p. 472-480.
14. Blackstock, D. Fundamentals of Physical Acoustics. John Wiley and Sons; 2000. p. 53-54.
15. Hambric S. Structural Acoustics Tutorial— Part 1: Vibrations in Structures. *Acoustics Today*. 2008; 2(4):21–33.
16. Hambric S, Fahnlne J. Structural Acoustics Tutorial—Part 2: Sound Structure Interaction. *Acoustics Today*. 2008; 3(2):9–27.
17. Kadam P, Kim J. Experimental Formulation of Four Poles of Three-dimensional Cavities and its Application. *Journal of Sound and Vibration*. 2007; 307:578–590.
18. Kim J, Soedel W. General Formulation of Four Pole Parameters for Three-Dimensional Cavities Utilizing Modal Expansion with Special Attention to the Annular Cylinder. *Journal of Sound and Vibration*. 1989; 129(2):237–254.

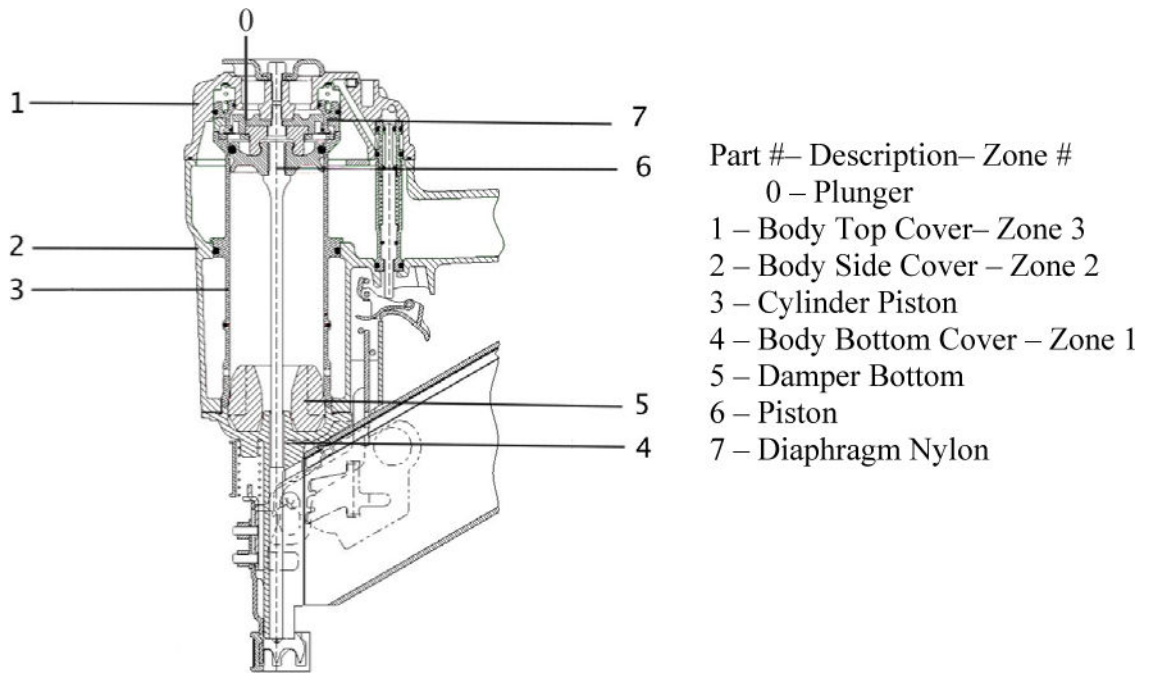


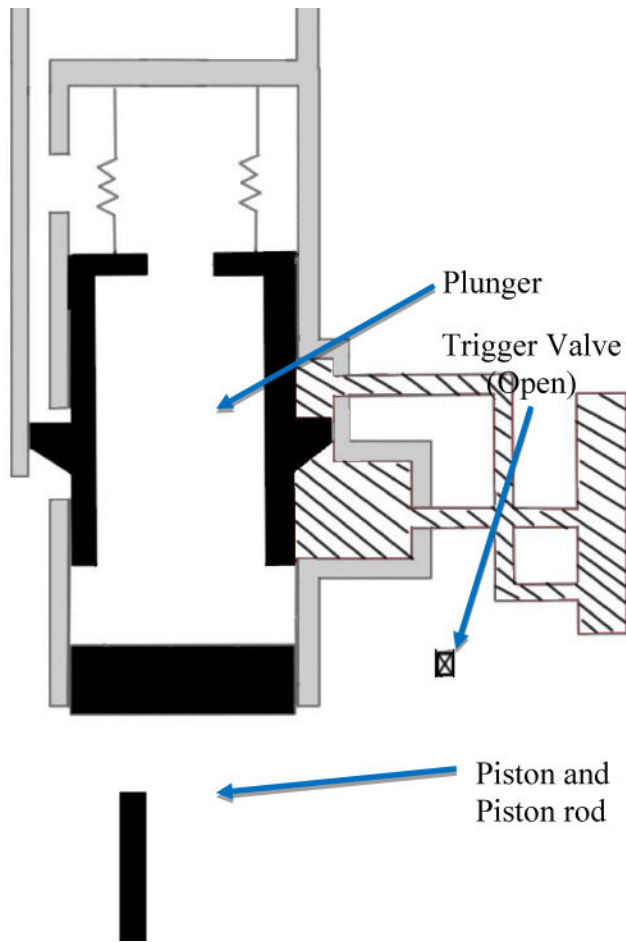
**Fig. 1.**  
Pneumatic nail gun cross section

Author Manuscript

Author Manuscript

Author Manuscript

Author Manuscript



Author Manuscript

Author Manuscript

Author Manuscript

Author Manuscript

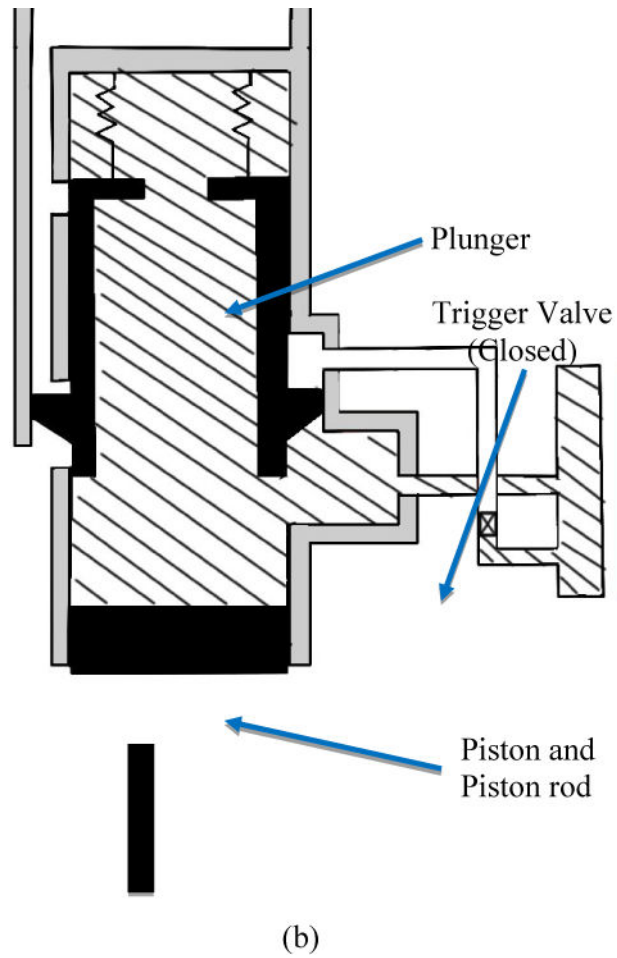


**Fig. 2.** Operating mechanism of a pneumatic nail gun. Figure 2 (a) shows the idle position. Sections shown in hatched indicate areas that the compressed air is filled. Figure 2 (b) Active status when trigger valve is closed and the piston is pushed toward the nail.

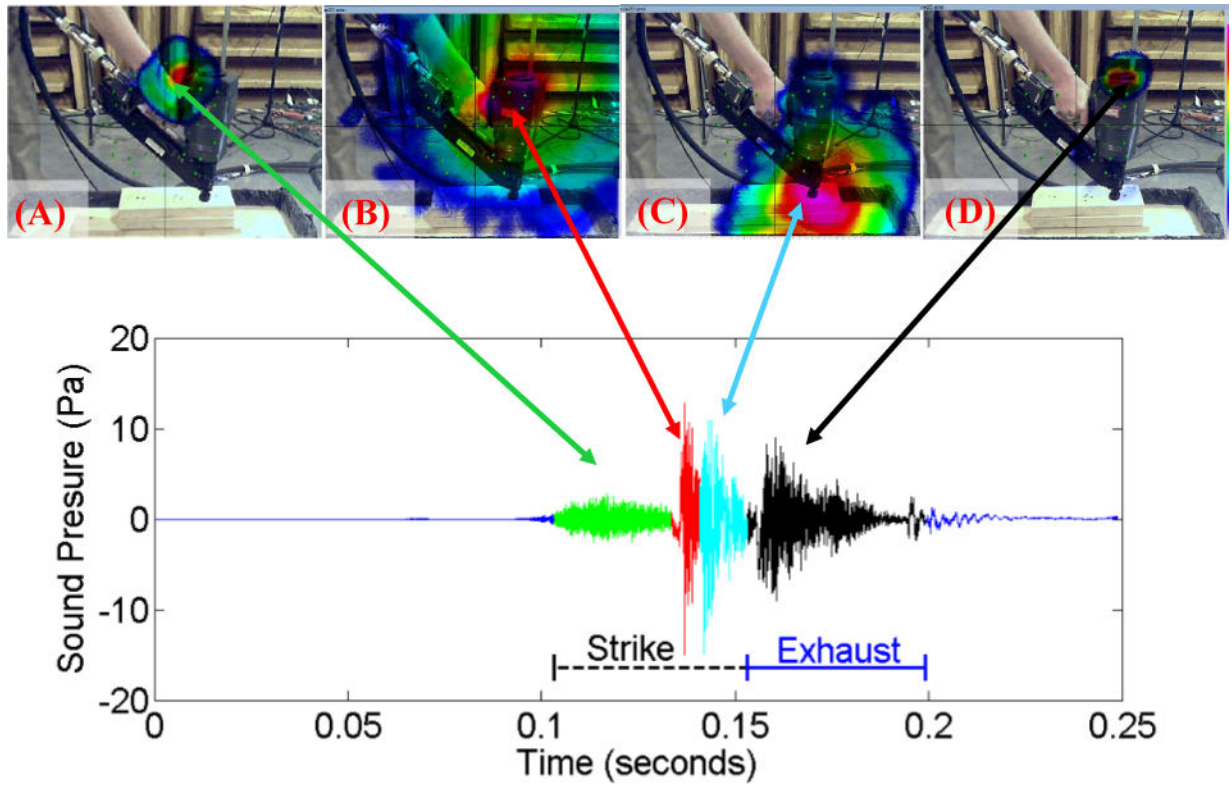


**Fig. 3.** Time history of the instantaneous pressure for a single fire of the nail gun. The strike event is within the dashed line on the left and exhaust event is within the solid-line on the right. The acoustic camera photos identify the noise sources during each cycle.



**Fig. 4.** Framing nailer test setup. Wooden two-2x4s are stacked in the sand box to receive the nails. The framing nailer operator made approximately ten measurements in position 1 and ten measurements in position 2.

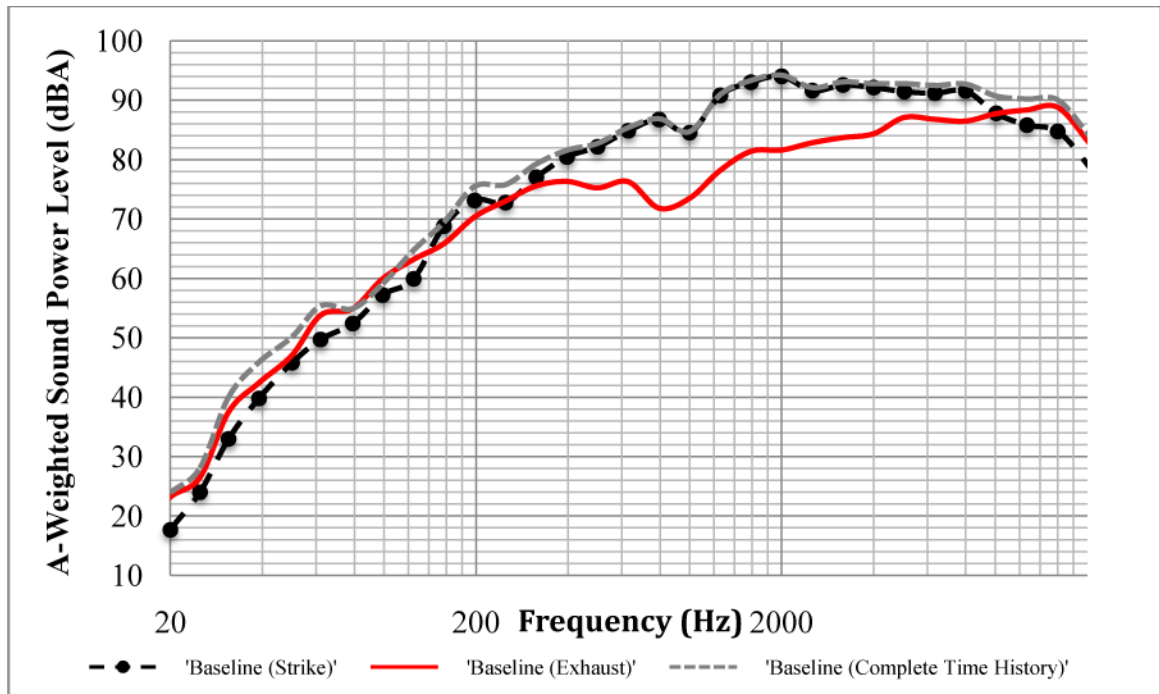
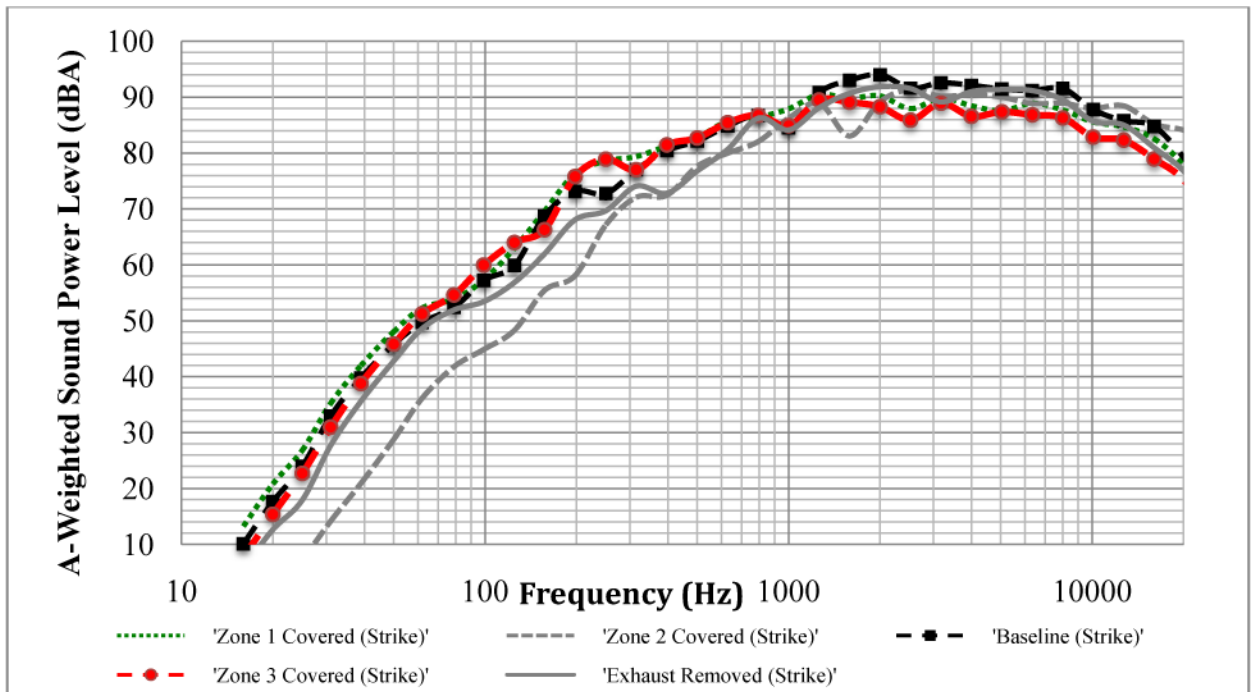
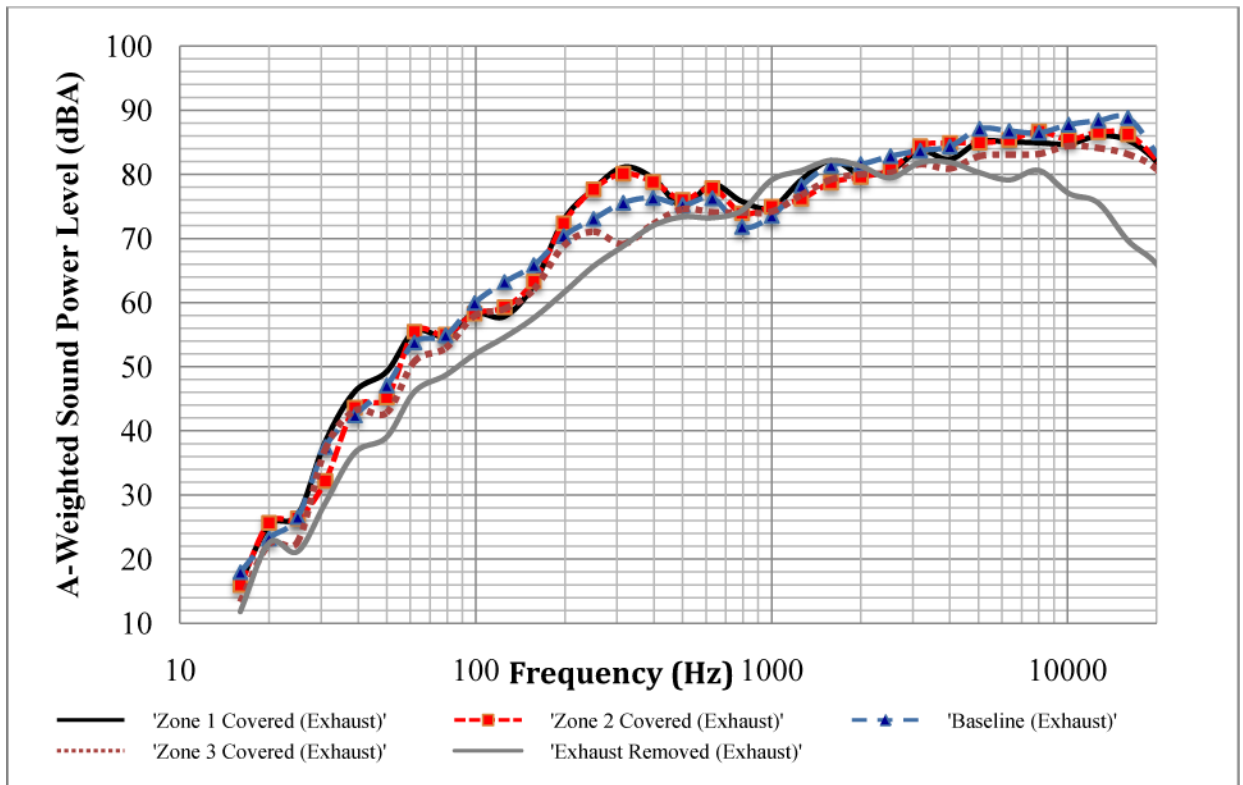


Fig. 5.  
A-weighted 1/3 octave band sound power level – Baseline



**Fig. 6.**  
A-weighted 1/3 octave sound power octave – Strike related noise



**Fig. 7.**  
A-weighted 1/3 octave sound power – Exhaust related noise

Muffler 1 TF

$$\begin{bmatrix} 1 & 0 \\ \frac{j\omega\rho_0 L_{e1}}{S_1} & 1 \end{bmatrix} \begin{bmatrix} 1 & \frac{jV_1\omega}{\rho_0 c^2} \\ 0 & 1 \end{bmatrix} \begin{bmatrix} 1 & 0 \\ \frac{j\omega\rho_0 L_{e2}}{S_2} & 1 \end{bmatrix}$$

Muffler 2 TF

$$\begin{bmatrix} 1 & \frac{jV\omega}{\rho_0 c^2} \\ 0 & 1 \end{bmatrix} \begin{bmatrix} 1 & 0 \\ \frac{j\omega\rho_0 L_{e2}}{S_2} & 1 \end{bmatrix}$$

Muffler 3 TF

$$\begin{bmatrix} 1 & 0 \\ \frac{j\omega\rho_0 L_{e1}}{S_1} & 1 \end{bmatrix} \begin{bmatrix} 1 & \frac{jV_1\omega}{\rho_0 c^2} \\ 0 & 1 \end{bmatrix} \begin{bmatrix} 1 & 0 \\ \frac{j\omega\rho_0 L_{e2}}{S_2} & 1 \end{bmatrix} \begin{bmatrix} 1 & \frac{jV_2\omega}{\rho_0 c^2} \\ 0 & 1 \end{bmatrix} \begin{bmatrix} 1 & 0 \\ \frac{j\omega\rho_0 L_{e3}}{S_3} & 1 \end{bmatrix}$$

Muffler 4 TF

$$\begin{bmatrix} 1 & 0 \\ \frac{j\omega\rho_0 L_{e1}}{S_1} & 1 \end{bmatrix} \begin{bmatrix} 1 & \frac{jV\omega}{\rho_0 c^2} \\ 0 & 1 \end{bmatrix} \begin{bmatrix} 1 & \frac{1}{Z_{as}} \\ 0 & 1 \end{bmatrix} \begin{bmatrix} 1 & 0 \\ \frac{j\omega\rho_0 L_{e2}}{S_2} & 1 \end{bmatrix}$$

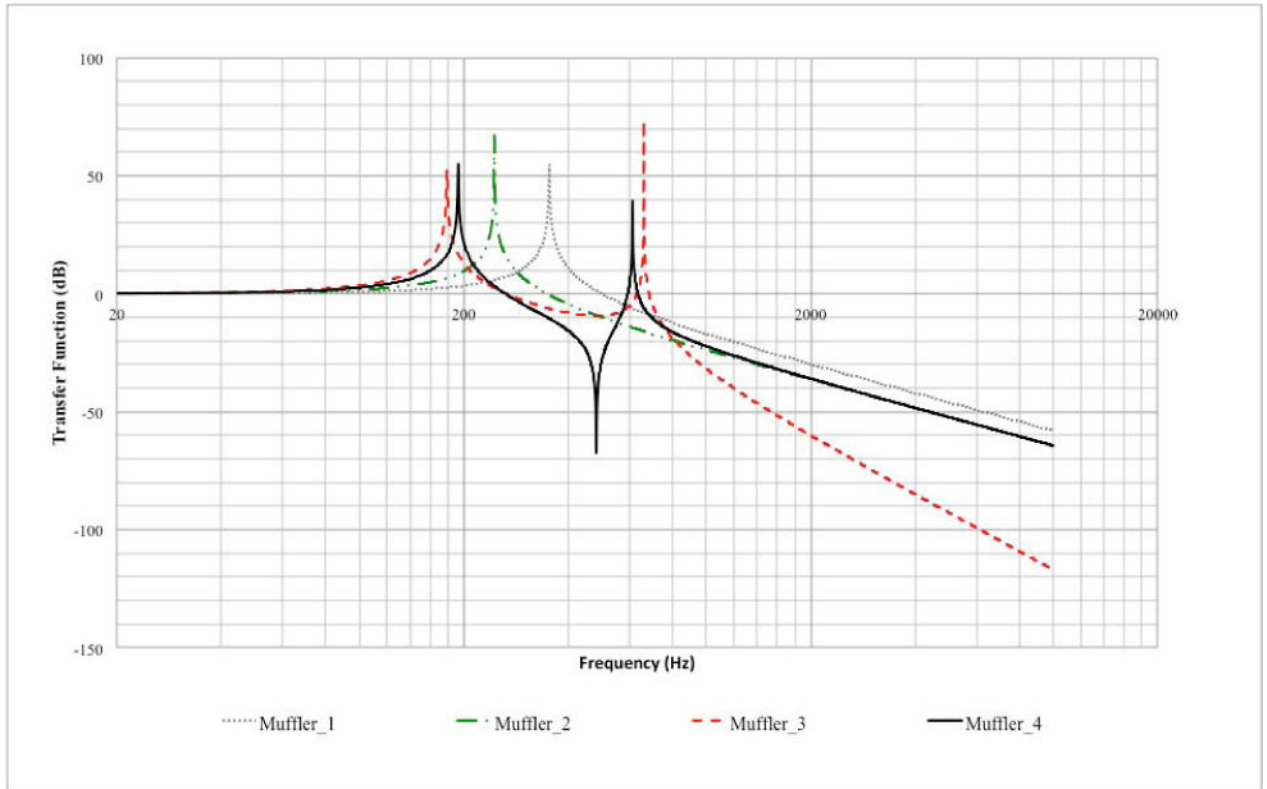


**Fig. 8.** Transfer function plot for muffler design comparison based on Eqn. 4-2

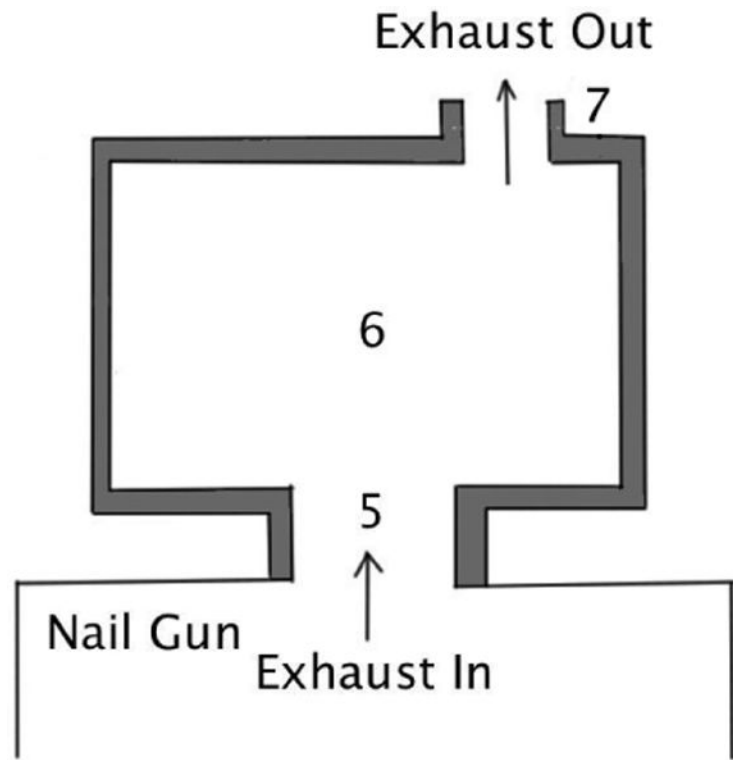


**Fig. 9.**  
Muffler design addressing only exhaust noise (Muffler 1)

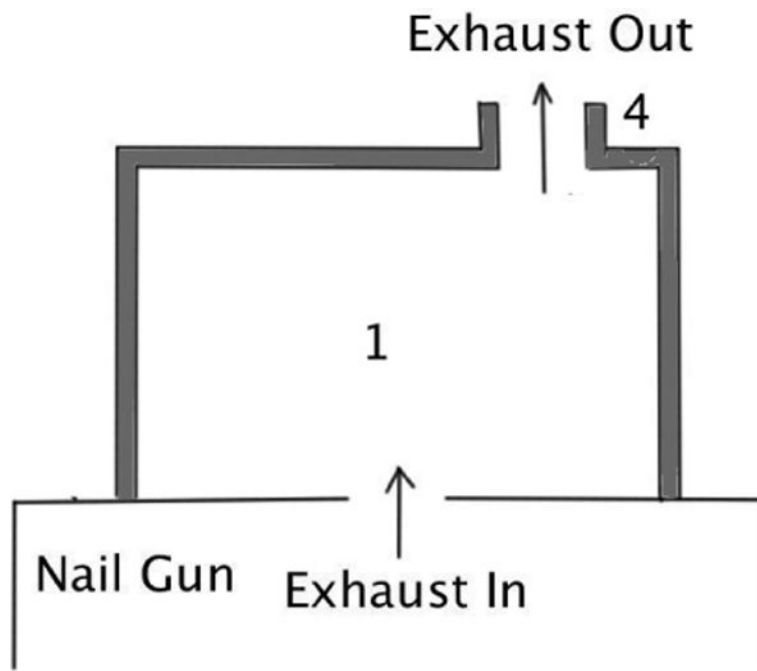


**Fig. 10.**  
Muffler design addressing structural and noise (Muffler 2)

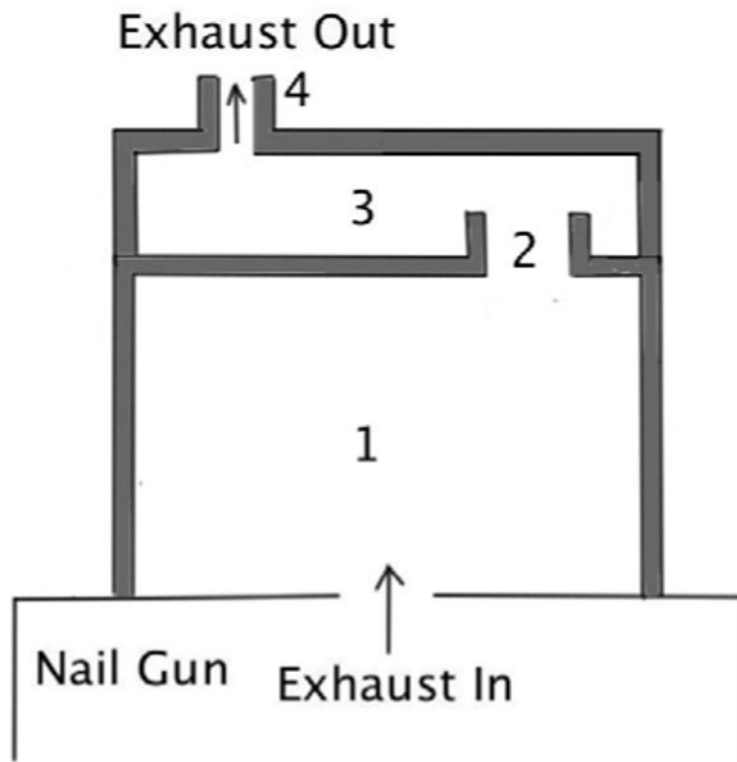


**Fig. 11.**  
Double chamber muffler design (Muffler 3)

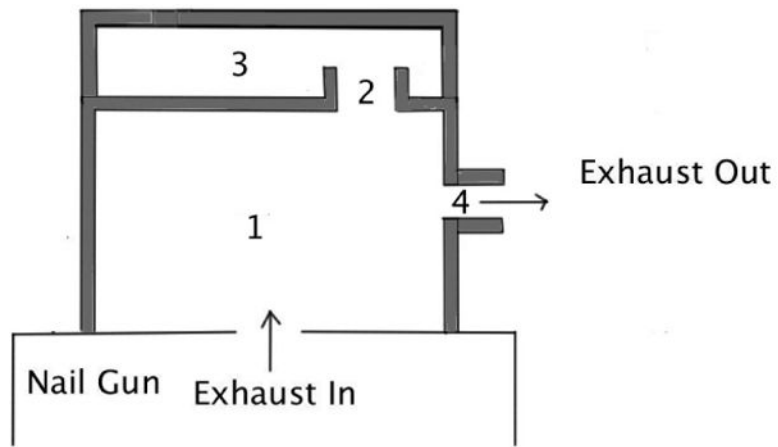


**Fig. 12.** Single chamber muffler design with resonator side branch (Muffler 4)

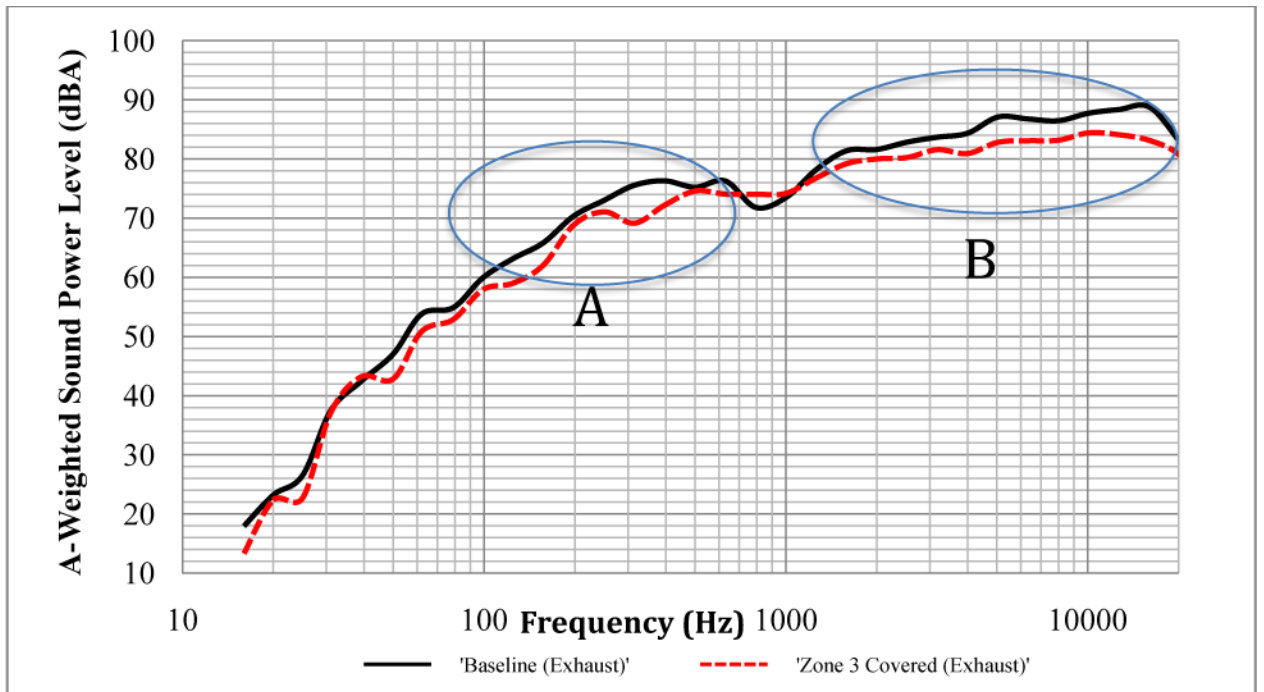


**Fig. 13.**  
A-weighted 1/3 octave band sound power level for only Zone 3 Covered

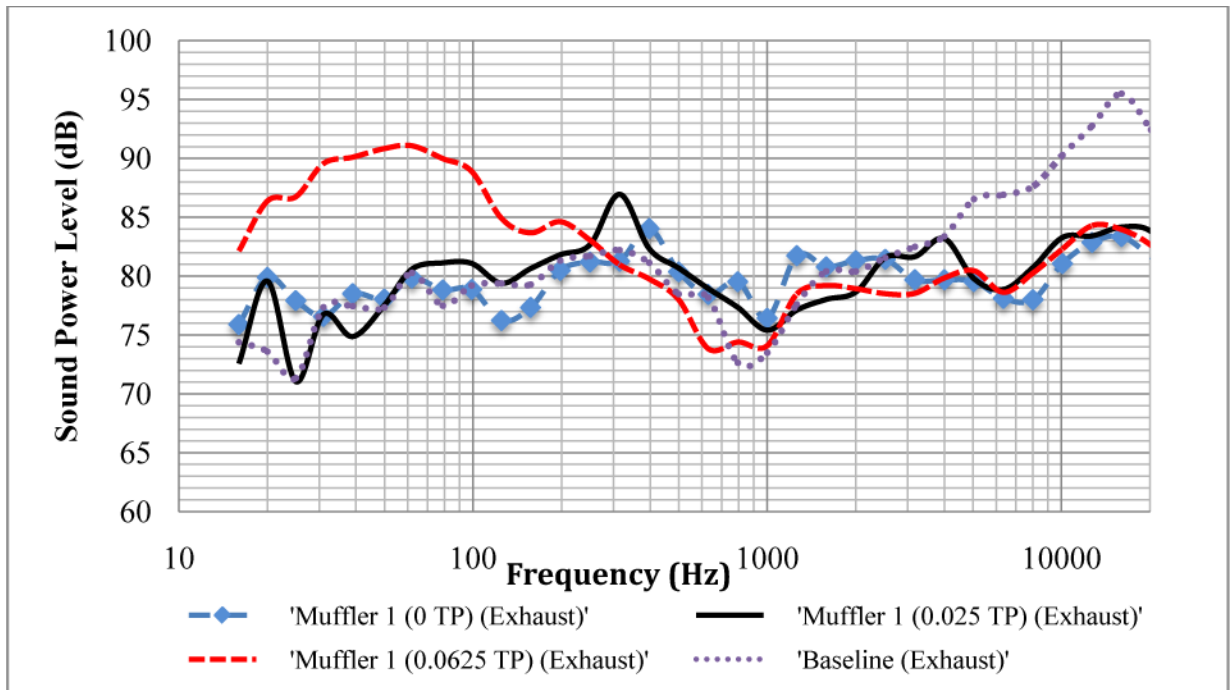


**Fig. 14.** Muffler 1 – Tail pipe length comparisons (A-weighted 1/3 octave sound power level)

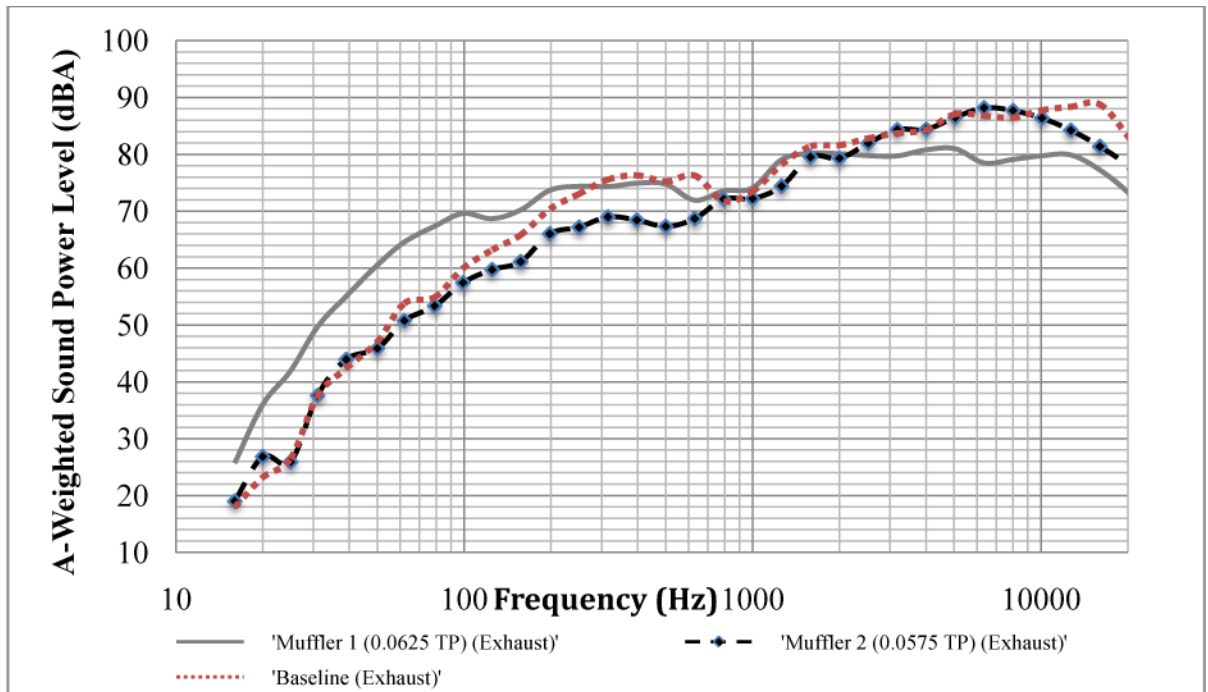


**Fig. 15.** Comparison of Muffler 1 and Muffler 2 (A-weighted 1/3 octave sound power level)

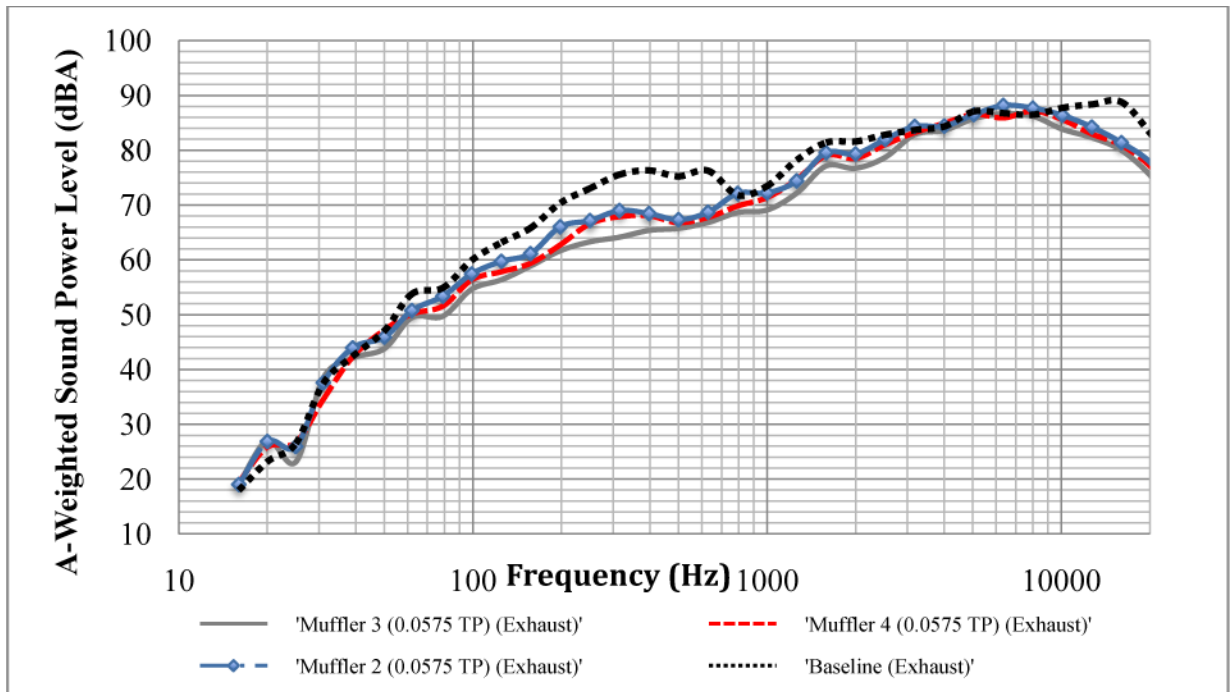


**Fig. 16.** Comparison of Muffler 2, Muffler 3 and Muffler 4 (A-weighted 1/3 octave sound power level)

**Table 1**

List of noise sources and transmission paths. Definitions of zones from Fig. 1 are Zone 1 – Body Bottom Cover, Zone 2 – Body Side Cover, and Zone 3 – Body Top Cover.

S.No	Source	Potential Paths
A	Compressed air flow through inlet port	Air borne noise from the trigger valve release
		Structure borne noise via Zone 2 and Zone 3
B	Piston Strike related mechanical impact processes	Air borne noise through the exhaust port
		Structure borne via Zone 1
		Structure Borne via Zone 2
C	Nail Striking Wood	Structure Borne via Zone 3
		Air Borne Noise from wood
		Air borne noise through the exhaust port
		Structure borne via Zone 1
D	Compressed air exhaust and mechanical impact from piston lodging back in its resting pad	Structure Borne via Zone 2
		Air borne noise through the exhaust port
		Structure borne via Zone 1
		Structure Borne via Zone 3

**Table 2**

Muffler design dimensions, element number corresponds to the number indicating muffler components in Figures 9 through 12. (The Figures 9 to 12 are representative and do not reflect the exact manner of implementation of the designs)

Element Number	Diameter (m)	Length (m)	Description
1	0.055	0.04	Small Volume
2	0.0125	0.025	Short Pipe
3	0.05	0.025	Small Volume
4	0.0125	0.0575	Short Pipe
5	0.03	0.03	Short Pipe
6	0.07	0.04	Small Volume
7	0.025	0/0.025/0.0625	Short Pipe

Author Manuscript

Author Manuscript

Author Manuscript

Author Manuscript

**Table 3**

Individual noise path isolation to estimate contribution to overall sound power

Case Name	Total Sound power Level (dBA)			Sources/Paths Isolated
	Strike	Exhaust	Strike+Exhaust	
Baseline	102.7	96.5	103.8	–
Exhaust Removed	101.2	90.8	101.8	Exhaust
Zone 1 covered	100.2	93.7	101.2	Zone 1
Zone 2 Covered	100.4	94.3	101.6	Zone 2
Zone 3 Covered	99.3	93.2	100.3	Zone 3 + Compressed Air Release from trigger valve
Muffler 1	101.5	92.9	102.0	Exhaust
Muffler 2	99.9	93.0	101.1	Exhaust + Zone 3
Muffler 3	100.3	91.1	100.8	Exhaust + Zone 3
Muffler 4	99.4	90.6	100.2	Exhaust + Zone 3